

## EXPERIMENTAL EVALUATION OF THE EM EXPOSURE IN THE SIMPLE ABDOMEN SOLID PHANTOM

Kazuya NAGASAWA<sup>1</sup>, Hiroki KAWAI<sup>1</sup>, Masaharu TAKAHASHI<sup>2</sup>, Kazuyuki SAITO<sup>2</sup>  
Koichi ITO<sup>2</sup>, Takuya UEDA<sup>3</sup>, Masayoshi SAITO<sup>3</sup>, Hisao ITO<sup>3</sup>  
Hisao OSADA<sup>4</sup>, Yoshio KOYANAGI<sup>5</sup>, and Koichi OGAWA<sup>6&2</sup>

<sup>1</sup>Graduate School of Science and Technology, Chiba University, 1-33 Yayoi-cho, Inage-ku, Chiba, 263-8522 Japan

<sup>2</sup>Research Center for Frontier Medical Engineering, Chiba University, 1-33 Yayoi-cho, Inage-ku, Chiba, 263-8522 Japan

<sup>3</sup>Graduate School of Medicine, Chiba University, 1-8-1 Inohana, Chuo-ku, Chiba, 260-8670 Japan

<sup>4</sup>Chiba University Hospital, 1-8-1 Inohana, Chuo-ku, Chiba, 260-8677 Japan

<sup>5</sup>Panasonic Mobile Communications Co., Ltd., 5-3 Hikirinooka, Kanagawa, 239-0847 Japan

<sup>6</sup>Matsushita Electric Industrial Co., Ltd., 1006 Kadoma, Osaka, 571-8501 Japan

E-mail: nagasawa@graduate.chiba-u.jp

### 1. Introduction

In the past few years, radiofrequency (RF) devices, which are usually used in the vicinity of the human body, are increasing. Therefore, it might be inferred that pregnant women and their fetuses are exposed to the electromagnetic (EM) waves radiated from the devices, e.g., portable radio terminals, induction heating cooker, hand-held metal detectors, etc.

Up to now, the authors have been investigated the evaluation of the EM waves' exposure in the pregnant women close to the portable radio terminals for business at 150 MHz [1]. It is supposed that EM waves of this device penetrate to the depths of the human body, because the wavelengths are longer than that of the cellular phone. Therefore, it is necessary to evaluate the EM exposure of the fetus in the abdomen model at the late pregnancy.

In this paper, we measure the temperature-rise distribution by the thermographic method using the simple abdomen solid phantom and a normal mode helical antenna (NHA) at 150 MHz, which replaces the portable radio terminals for business, and compared with calculated result by the FDTD method.

### 2. Model and condition

#### 2.1 Experimental model

Figure 1 illustrates the structure of the simple abdomen model, which is composed by three tissues of the mother's body, amniotic fluid (AF), and fetus, based on MRI tomograms of pregnant women. From these data, the measurements of the maximum width, height, position of these tissues is evaluated. In addition, as shown in Fig. 1, the AF and the fetus are modeled by ellipsoids. Fig. 2 shows a simple abdomen phantom which is developed on the basis of Fig. 1.

Figure 3 shows a  $0.11\lambda$  NHA, which simulates the actual portable radio terminals at 150 MHz, close to a simple abdomen model. Here, the antenna is attached close to in front of the abdomen to consider the worst case of the exposure inside the fetus. In addition, the distance between the antenna and the surface of the human model is constantly 40 mm to realize the actual situation. Moreover, the origin is the feed point of the antenna. Fig. 3 (b) illustrates the observation plane and line of the temperature-rise distribution. Here, the observation line is directly under the feed point along the  $y$ -axis on the  $x$ - $y$  plane ( $z=0$ ).

Table I describes the parameters of the tissues. Here, the electrical properties of the human body consist of a mixture of the human body tissues (2/3 muscles) [2]. These parameters are the measured values of the phantom. In addition, the target value of the electric constants at the AF uses the measured value of the healthy human's AF. And ones at the fetus use the measured value of the white rabbit's fetus.

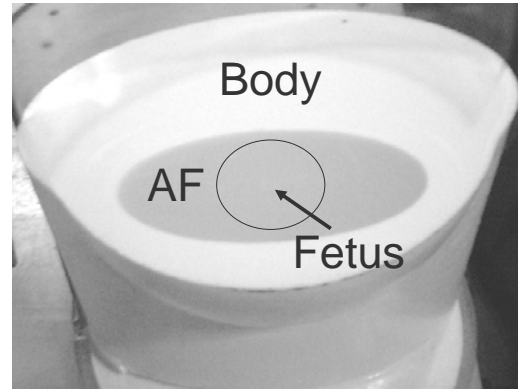
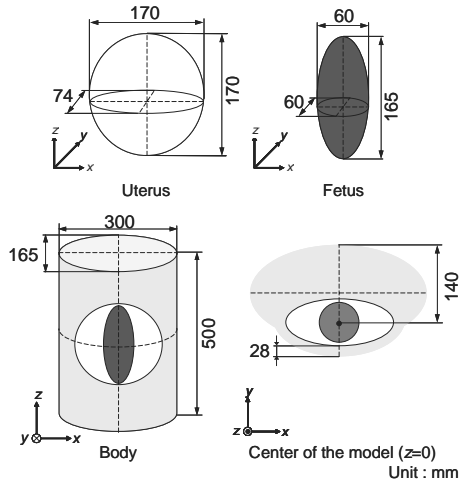


Fig. 1 Simple abdomen model of pregnant women. Fig. 2 Simple abdomen phantom (half cut).

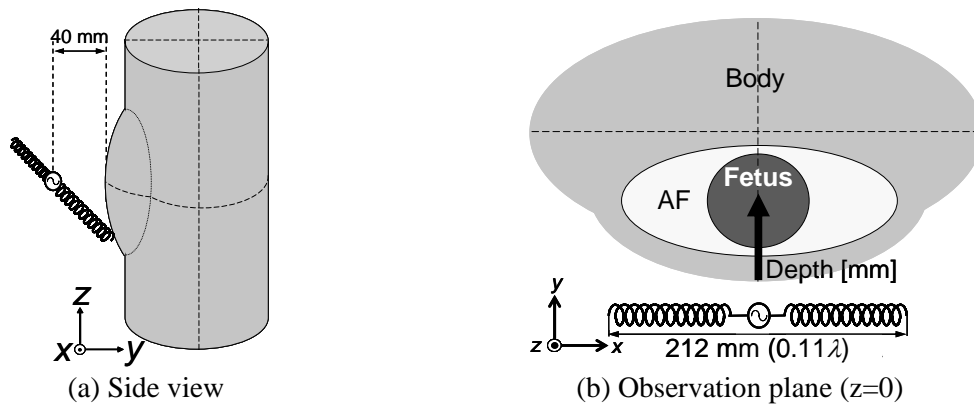


Fig. 3 Experimental and numerical model.

Table I Electric constants and density of tissues

	Body	AF	Fetus
Relative permittivity $\epsilon_r$	42.1	78.3	76.9
Conductivity $\sigma$ [S/m]	0.50	1.23	0.91
Density $\rho$ [kg/m <sup>3</sup> ]	907	986	967

## 2.2 Thermographic method

The thermographic method is one of the SAR evaluation method [3], [4]. This method is based on the thermal measurement. In addition, this method uses an infrared camera and a tissue-equivalent solid (gel) phantom. Here, the exposure time must be as short as possible within a range that makes the heat distribution observable, to minimize the heat diffusion. If the heat diffusion and exposure time are negligibly small, the SAR at an arbitrary point is given directly by

$$\text{SAR} = c \frac{\Delta T}{\Delta t} \quad [\text{W/kg}] \quad (1)$$

where,  $c$  is the specific heat of the phantom [J/kg/K],  $\Delta T$  is the temperature-rise in the phantom [K], and  $\Delta t$  is the exposure time [s].

## 2.3 Measurements

The temperature-rise distribution is measured in the radio anechoic chamber in Chiba University. Temperature of this room was 18 degrees. The infrared camera used for the measurement is TH3102MR manufactured by the NEC Sanei Co., Ltd, Tokyo, Japan.

As the procedure for the measurement, at first, it laps two simple abdomen models, sets up a NHA as shown in Figure 3 (a), and radiates the EM waves from a NHA to the simple abdomen models at the short time. Second, it takes off the simple abdomen models after NHA radiated the EM waves. Finally, it measures the temperature-rise of the observation plane at the lower part of simple abdomen model using the infrared camera.

As the condition of the EM exposure, the input power of the antenna is 94 W and the exposure time is 180 s. The high power is necessary to realize the accurate measurements. In addition, an emittance of the simple abdomen model is 0.84.

## 2.4 Thermal analysis

This analysis uses The FDTD method. The FDTD software (SEMCAD ver. 1.6 [5]) is used for the SAR calculating in the simple abdomen models. The parameters of the FDTD calculation employed in this Section are as follows: the minimum cell size of the NHA is 0.5 mm; the cell size of the abdomen model is 0.5-10 mm; the cell size of free space is 0.5-20 mm; the absorbing boundary condition is the PML (eight layers).

Next, the thermal solver, which is including SEMCAD, is used for the thermal analysis in the abdomen model. Table II describes the thermal properties of the phantoms. The temperature-rise distribution inside the phantom could be calculated by solving this equation

$$\rho c \frac{\partial T}{\partial t} = \kappa \nabla^2 T + \rho \cdot \text{SAR} \quad (2)$$

where  $T$  is the temperature of the tissue [K],  $t$  is the time [s],  $\kappa$  is the thermal conductivity [W/m/K].

In addition, the boundary conduction for Eq. (2) is given by the following equation

$$h(T - T_a) = \kappa \frac{\partial T}{\partial n} \quad (3)$$

where  $h$  is the heat transfer coefficient [W/m<sup>2</sup>/K],  $T_a$  is the temperature of the air around the phantom [K], and  $\partial T/\partial n$  the variation in the temperature toward normal from the phantom surface. Therefore, the temperature-rise inside the phantom can calculate by solving Eqs. (2) and (3).

The conditions of the thermal analysis are as follows: the initial temperature of the phantoms and the air is 18 degrees to realize the actual measurement; the heat transfer coefficient  $h$  is 20 W/m<sup>2</sup>K to realize the condition of the radio anechoic chamber in Chiba University; the output power of the antenna is 94 W; the exposure time is 180 s.

Table II Thermal constants of tissues

	Body	AF	Fetus
$c$ [J/kg/K]	3,060	4,010	4,030
$\kappa$ [W/m <sup>2</sup> /K]	0.36	0.67	0.61

## 3. Results

Figure 4 shows the temperature-rise distribution on the observation plane. As shown in Figs. 4 (a) and (b), the measured result is in good agreement with the calculated one. In addition, it is confirmed the EM waves penetrate the inside of the model with the current distribution of a NHA. Moreover, the maximum temperature-rise occurs in the right and left of model's surface to be antenna near field of a NHA.

Figure 5 shows the temperature-rise distribution on the observation line. As shown in Fig. 5, there is confirmed the difference occurs between the measured result and the calculated one at the body's surface. However, the error is small to difference of two results is at 0.5 degrees. In addition, two results show almost the similar tendency. Therefore, the measured one is in good agreement with the calculated one.

Figure 6 shows the SAR distribution on the observation line. The measured result changes from Fig. 5 to the SAR using Eq. (1). As a result, the difference causes between measured one and

calculated one at the body region and around the boundary between two tissues. Therefore, it is necessary to revise this error to be the validity evaluation.

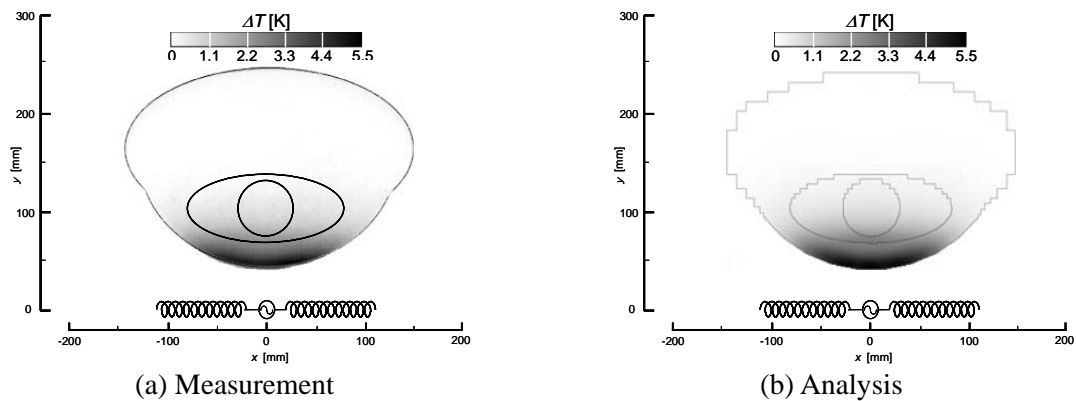


Fig. 4 Temperature-rise distributions in the observation plane

(The cell of the model is small in the vicinity of a NHA and is rough in the far distance in Fig. 4(b)).

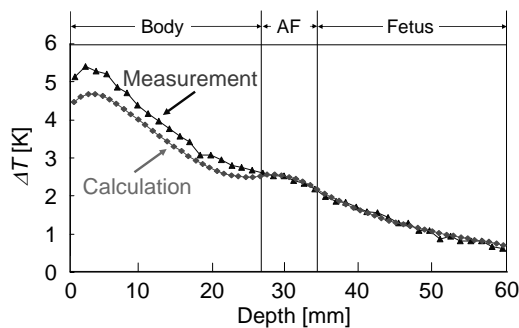


Fig. 5 Temperature-rise distributions on the observation line.

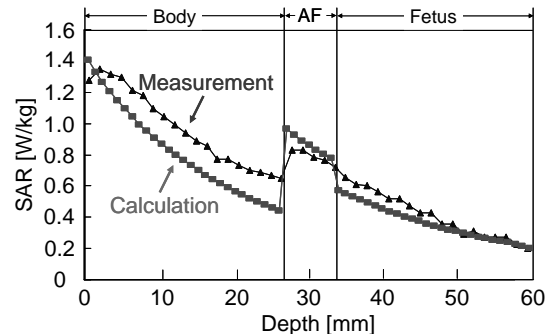


Fig. 6 SAR distributions on the observation line.

#### 4. Conclusion

In this paper, we investigated the temperature-rise distribution inside the simple abdomen model of the pregnant women, which was close to the portable radio terminals at 150 MHz. As a result, the measured temperature-rise distribution is in good agreement with the calculated one. However, the SAR one causes the difference between measured one and calculated one at the body region and around the boundary between two tissues. Therefore, it is necessary to revise this error to be the validity evaluation.

In near future, we study the way to revise the error between the SAR distribution of the measurement and that of the calculation.

#### References

- [1] K. Ito, H. Kawai, M. Takahashi, *et al*, "Evaluation of the local SAR in a simple abdomen model of pregnant women at 150 MHz," *Biological EM meeting* (Dublin, Ireland), June 2005, BEMS 2005 to be published.
- [2] Y. Koyanagi, H. Kawai, K. Ogawa, H. Yoshimura and K. Ito, "Estimation of the radiation and SAR characteristics of the NHA at 150 MHz by use of the cylindroid whole body phantom," *Proc. 2001 IEEE APS* (Boston, USA), vol. 3, pp. 78-81, July 2001.
- [3] A. W. Guy, "Analysis of electromagnetic fields induced in biological tissues by the thermographic studies on equivalent phantom models," *IEEE Trans. Microwave Theory Tech.*, vol. 19, no. 2, pp. 205-214, Feb. 1971.
- [4] Y. Okano, K. Ito, I. Ida, and M. Takahashi, "The SAR evaluation method by a combination of thermographic experiments and biological tissue-equivalent phantoms," *IEEE Trans. Microwave Theory Tech.*, vol. 48, no. 11, pp. 2094-2103, Nov. 2000.
- [5] Schmid & Partner Engineering AG web site (<http://www.speng.com/>).